BIOCHEMISTRY
including biophysical chemistry & molecular biology

Article

pubs.acs.org/biochemistry

Peptides as Inhibitors of the First Phosphorylation Step of the *Streptomyces coelicolor* Phosphoenolpyruvate: Sugar Phosphotransferase System

Rosa Doménech,[†] Sergio Martínez-Rodríguez,[‡] Adrián Velázquez-Campoy,*[,§,∥,⊥] and José L. Neira*[,†,§]

[†]Instituto de Biología Molecular y Celular, Universidad Miguel Hernández, Elche (Alicante), Spain

[‡]Departamento de Química-Física, Bioquímica y Química Inorgánica, Universidad de Almería, Almería, Spain

[§]Instituto de Biocomputación y Física de Sistemas Complejos (BIFI), Unidad Asociada IQFR-BIFI, Universidad de Zaragoza, Zaragoza, Spain

[∥]Fundación ARAID, Diputación General de Aragón, Zaragoza, Spain

[⊥]Departamento de Bioquímica y Biología Molecular y Celular, Universidad de Zaragoza, Zaragoza, Spain

Supporting Information

ABSTRACT: The phosphotransferase system (PTS) controls the use of sugars in bacteria. The PTS is ubiquitous in bacteria, but it does not occur in plants and animals; it modulates catabolite repression, intermediate metabolism, gene expression, and chemotaxis. Its uniqueness and pleiotropic function make the PTS an attractive target for new antibacterial drugs. The PTS is constituted of two general proteins, namely, enzyme I (EI) and the histidine phosphocarrier (HPr), and various sugar-specific permeases. EI has two domains: the N-terminal domain (EIN), which binds to HPr, and the C-terminal domain (EIC), which contains the dimerization interface. In this work, we determined the binding affinities of peptides derived from EIN of *Streptomyces coelicolor* (EIN^{sc}) against HPr of the same organism (HPr^{sc}), by using nuclear magnetic resonance and isothermal titration calorimetry techniques. Furthermore, we measured the affinity of EIN^{sc} for (i) a peptide derived from HPr^{sc}, containing the active-site histidine, and (ii) other peptides identified previously by phage display and combinatorial chemistry in *Escherichia coli* [Mukhija, S. L., et al (1998) *Eur. J. Biochem.* 254, 433−438; Mukhija, S., and Erni, B. (1997) *Mol. Microbiol.* 25, 1159−1166]. The affinities were in the range of ∼10 μM, being slightly higher for the binding of EIN^{sc} with peptides derived from HPr^{sc}, phage display, or combinatorial chemistry (K_D ∼ 5 μM). Because the affinity of intact EIN^{sc} for the whole HPr^{sc} is 12 μM, we suggest that the assayed peptides might be considered as good hit compounds for inhibiting the interaction between HPr^{sc} and EIN^{sc}.

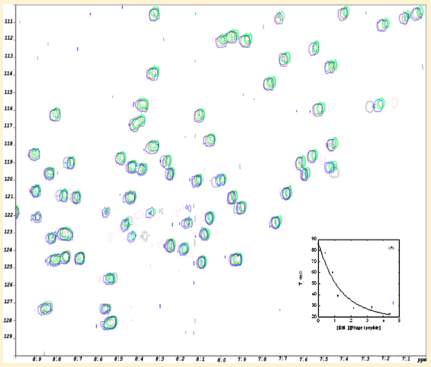

The bacterial phosphoenolpyruvate (PEP):sugar phosphotransferase system modulates the preferential use of carbon sources in bacteria. It is involved in (i) the transport and the uptake of several carbohydrates through the cell wall, (ii) the cell movement toward the carbon sources (chemotaxis), and (iii) the regulation of other metabolic pathways in both Gram-negative and Gram-positive bacteria.[1−4] The basic composition of the PTS is similar in all species described so far; it consists of a cascade of phosphoryl-transfer stages from PEP to the sugar-specific enzyme II permeases (EIIs). The first two proteins in the cascade are common to all PTS substrates: phosphocarrier enzyme I (EI) and histidine phosphocarrier (HPr) proteins. In the first step of the PTS, EI is phosphorylated by PEP in the presence of Mg^{2+}; subsequently, the phosphoryl group is transferred to HPr.[2,5] HPr is able to transfer the phosphate group to the active site of an EII permease (usually, but not exclusively, at a histidine residue). EI is at the top of the PTS cascade, and by using PEP, it links the PTS with glycolysis.[1,2] Therefore, any compound inhibiting EI should have a pleiotropic effect, interrupting the phosphorylation, and uncoupling the phosphorylation cascade from other catabolic routes; depletion of PEP, interruption of carbohydrate transport, and repression of some genes could compromise cell growth and infectivity. Therefore, we suggest that the first phosphorylation step in the PTS may represent an important drug target for altering cell growth.

Sequence comparisons among EIs and HPrs from several organisms reveal significant identity.[6] The 64 kDa EI protein in the species described so far is a homodimer. Proteolytic cleavage of EI^{ec} yields two domains.[7] The EIN comprises, roughly, the first 230 residues of the protein: it contains the HPr-binding domain and the active-site histidine.[5] The EIC mediates dimerization and binds PEP in the presence of Mg^{2+}.[8,9] The structure of EIN^{ec} has been determined by X-ray and nuclear magnetic resonance (NMR),[10,11] and its complex with HPr^{ec} has been characterized by NMR techniques.[12] The

Received: June 15, 2012
Published: August 21, 2012

isolated EIN^{ec}, which consists of an α-helix and an α/β domains, is structurally similar to the phospho-histidine domain of the pyruvate-phosphate dikinase.[13]

Streptomyces is a soil-dwelling Gram-positive actinomycete, with a high content of G and C, that grows on a variety of carbon sources. The complete genome of *Streptomyces coelicolor* has been sequenced, and the different components of the PTS have been reported.[14−16] Previously, we have undertaken an extensive description of the structures and conformational stabilities of the HPr^{sc} and EI^{sc} proteins, as a first step in understanding their binding reaction.[17−20] In addition, we have also measured the affinity constant of a small peptide derived from HPr^{sc}, containing the active-site histidine (His15), HPr^{9-30}, toward the entire EI^{sc}; the affinity constant is ∼200 μM, lower than that measured for the intact HPr^{sc} (∼100 μM).[21] In this work, we went a step further (i) to select a peptide derived from the HPr^{sc} sequence that was able to bind EIN^{sc} and (ii) to design peptides derived from the EIN^{sc} sequence that were able to bind HPr^{sc}. In addition, we measured the affinity of EIN^{sc} for peptides derived from phage display studies or from support-based combinatorial libraries, which are able to bind EI^{ec}.[22,23] By using EIN^{sc}, instead of the whole dimeric EI^{sc}, the protein−peptide binding reaction is not complicated by the dimerization equilibrium of EI^{sc}. The results show that the affinity of the EIN^{sc}-derived peptides for HPr^{sc} was ∼10 μM, similar to that measured for the EIN^{sc}−HPr^{sc} interaction [12 μM (unpublished results)]. On the other hand, the affinities of HPr-derived, phage, and combinatorial peptides for EIN^{sc} were higher (∼8 μM) than that measured for the HPr^{9-30}−EI^{sc} complex (∼200 μM[21]), suggesting that dimerization of EI^{sc} affects peptide binding; furthermore, the affinity of these peptides was slightly higher than that between EIN^{sc} and HPr^{sc}. Interestingly enough, most of the peptides showed antimicrobial activity in vivo. Taken together, these results indicate that (i) these peptides might be considered as hit compounds against inhibition of EI^{sc} and (ii) peptides derived from binding to the PTS proteins of a bacterial species can be used against the PTS proteins of other organisms.

MATERIALS AND METHODS

Materials. Deuterium oxide and deuterated Tris were obtained from Apollo Scientific (Stockport, U.K.), and TSP was from Sigma (Barcelona, Spain). The Ni^{2+} resin was from GE Healthcare (Barcelona, Spain). Dialysis tubing (SpectraPor), with a molecular mass cutoff of 3500 Da, was from Spectrum Laboratories (Japan). Standard suppliers were used for all other chemicals. Water was deionized and purified on a Millipore system.

Protein Expression and Purification. EI^{sc}, EIN^{sc}, and HPr^{sc} were purified as described previously.[17,19,24] The ^{15}N-labeled HPr^{sc} was prepared by growing *Escherichia coli* C41 cells[25] in M9 minimal medium as described previously;[26] protein purification was similar to that of the unlabeled protein.[17] Protein concentrations were determined from the absorbance of individual amino acids[27] at 280 nm, by using a Shimadzu UV-1601 spectrophotometer, in a 1 cm path length cell (Hellma).

Peptide Selection and Design. We followed a two-part approach. First, we selected peptides that were able to bind EIN^{sc}, and second, we designed peptides that were able to bind HPr^{sc}. All peptides were purchased from Genscript; purity was confirmed by mass spectrometry and sodium dodecyl sulfate.

Peptides That Are Able To Bind EIN^{sc}. The HPr^{9-30} peptide (GWAEGLHARPASIFVRAATATG-amidated) was derived from HPr^{sc}, spanning residues Gly9−Gly30. Those amino acids belong to the first α-helix of HPr^{sc} (residues Ala16−Thr27, in the numbering of the intact protein) and the preceding loop containing the active-site histidine and three flanking residues on each side to avoid fraying effects. We have previously assayed this peptide against the whole EI^{sc}, and its affinity is ∼200 μM.[21]

We also studied peptide Phage1 (GLRFGKTRVHYLVLG-amidated), derived from phage display studies against EI^{ec}, which has a small IC_{50} inhibition constant (25 μM),[23] and Phage2 (KKWHLRKR-amidated), derived from support-based combinatorial libraries, which has a small inhibition IC_{50} (30 μM).[22] Both peptides are positively charged, and they contain a His residue, which is the putative active site.

Peptides That Are Able To Bind HPr^{sc}. We have used our previous modeled structure of EIN^{sc} [20] and the structure of EIN^{ec}−HPr^{ec} complex[12] to design the peptides. Two different peptides were designed: (i) the so-called EINbsite (FVTEEGGPTSHSAILARA-amidated), containing the active-site histidine of EIN^{sc} (His186) and comprising half of the sixth α-helix of EIN^{sc},[20] and (ii) the so-called EINosite (YRALLA-GAGEYLAGRVADLDD-amidated), comprising half of the third α-helix, the in-between loop, and half of the fourth α-helix of the intact EIN^{sc},[20] which shows contacts with the active-site region of HPr^{ec} in the EIN^{ec}−HPr^{ec} complex.[12]

Isothermal Titration Calorimetry. ITC measurements were performed by using a VP-ITC isothermal titration calorimeter (MicroCal, Northampton, MA). Two different binding experiments were conducted.

Measuring the Affinity of Synthetic Peptides for EIN^{sc}. We conducted the binding reactions between EIN^{sc} and HPr^{9-30}, Phage1, and Phage2 peptides. The sample cell (1.4 mL) was loaded with EIN^{sc} (at a concentration of 20 μM); the syringe was loaded with the corresponding peptide (at a concentration of ∼400 μM).

Measuring the Affinity of Synthetic Peptides for HPr^{sc}. We conducted binding experiments involving HPr^{sc} and EINosite and EINbsite peptides (and also with an equimolar mixture of both peptides). The sample cell (1.4 mL) was loaded with HPr^{sc} (at a concentration of 20 μM); the syringe was loaded with the corresponding peptide (at a concentration of ∼400 μM; in the peptide cocktail, the concentration of each EINsite peptide was also 400 μM).

In all the assays, a total of 28 injections of 10 μL were added sequentially to the sample cell after a 400 s spacing to ensure that the thermal power returned to the baseline before the next injection. The amount of thermal power required to maintain the reaction cell at a constant temperature after each injection was monitored as a function of time. The isotherms (differential heat upon binding vs the molar ratio of the compounds in the cell) were fit to a single-site model assuming that the complex has a 1:1 stoichiometry. Data were analyzed with software developed in our laboratory, implemented in Origin 7.0 (OriginLab).

To determine the buffer-independent enthalpy of the binding reaction, the effect of the buffer ionization heat was taken into account by conducting the binding reaction in two buffers: (a) 10 mM Tris (pH 7) and (b) 10 mM Mops (pH 7), which have different ionization enthalpies, ΔH_{ion} (11.7 and 5.5 kcal mol^{-1}, respectively). With this procedure, the buffer-independent enthalpy of the binding reaction, $\Delta H°$, and the number of

dx.doi.org/10.1021/bi3010494 | *Biochemistry* 2012, 51, 7393−7402

exchanged protons between the complex and the bulk solution, n_H, were calculated. The apparent enthalpy change, $\Delta H_{meas;buffer}$, in the corresponding buffer is[28]

$$\Delta H_{meas,buffer} = \Delta H^\circ + n_H \Delta H_{ion} \quad (1)$$

A positive value of n_H indicates a net protonation, and a negative value of n_H indicates a net deprotonation. The value of n_H depends on the number of functional ionizable groups involved in the proton exchange and whose pK_a changes significantly upon formation of the protein−peptide complex. The expression for n_H is

$$n_H = \sum_{i=1}^{m} \left(\frac{10^{pK^C_{a,i}-pH}}{1 + 10^{pK^C_{a,i}-pH}} - \frac{10^{pK^F_{a,i}-pH}}{1 + 10^{pK^F_{a,i}-pH}} \right) \quad (2)$$

where m is the number of ionizable groups and $pK^C_{a,i}$ and $pK^F_{a,i}$ are the pK_a values for ionizable group i in the complex (C) and free (F) states, respectively. Ionizable groups involved may belong to the protein or the peptide. Therefore, n_H is the difference in the proton saturation fraction of the ionizable groups in the complex and the free state. It is obvious that if either (1) $pK^C_{a,i}$ and $pK^F_{a,i}$ are very similar or (2) $pK^C_{a,i}$ and $pK^F_{a,i}$ are different but very far from the experimental pH, the ionizable group does not contribute to the n_H value. In addition, n_H is related to the pH dependency of the association constant (or binding affinity), according to

$$n_H = -\frac{\partial(\log K_a)}{\partial(pH)} \quad (3)$$

According to eqs 2 and 3, n_H may take fractional values. For example, let us assume that pH = 7, and there is just one ionizable group with a pK^C_a of 5.5 and a pK^F_a of 6.5 (this may be a histidine residue with a pK_a of 6.5 in the free protein that undergoes a reduction in pK_a upon ligand binding). Then, according to eq 2, $n_H = 0.03 - 0.24 = -0.21$, and this result cannot be interpreted as if each of these histidine residues releases 0.21 proton, but that, "on average", each of these histidine residues releases 0.21 proton (that is, some histidines will release a proton and some will not). In fact, $n_H = 0.03 - 0.24 = -0.21$ means that in the free protein these histidine residues exhibit a proton saturation fraction of 0.24 (that is, 24% of these histidine residues are protonated in the free protein) and that in the complex these histidine residues exhibit a proton saturation fraction of 0.03 (that is, 3% of these histidine residues are protonated in the complex), because of a reduction in pK_a upon formation of the complex. As a consequence of formation of the complex, protons are released to the bulk solvent.

The change in heat capacity on binding (ΔC_p) was calculated from the enthalpy values obtained at different temperatures by using the buffers described.

NMR Spectroscopy. The NMR experiments were conducted in a Bruker Avance DRX-500 spectrometer (Bruker GmbH), equipped with a triple-resonance probe and z-pulse field gradients. Processing of spectra was conducted with XWINNMR. TSP was used as the external chemical shift reference, and the ^{15}N dimension of the two-dimensional (2D) heteronuclear single-quantum coherence (HSQC) spectra was referenced indirectly.[29]

One-Dimensional NMR Experiments. Water was suppressed with the WATERGATE sequence.[30] Usually, 512 scans were acquired with a spectral width of 12 ppm, with 16K data points in the time domain. The data matrix was zero-filled to 32 K during processing. Experiments were conducted in 50 mM phosphate buffer (pH 7.0); the lyophilized peptides (at 100 μM) were dissolved in a 90% H_2O/10% D_2O mixture.

2D Homonuclear Experiments. Common TOCSY, ROESY, and NOESY experiments[31] were conducted as described previously[32] at 10 °C in aqueous solution to assign Phage1, Phage2, EINbsite, and EINosite peptides. Concentrations were in all cases ~2 mM. Typically, 200 experiments, with 160 scans for the NOESY and ROESY experiments and 80 scans for the TOCSY experiments, were conducted with 4K points in the F_2 dimension. The mixing times for the NOESY, ROESY, and TOCSY experiments were 200, 200, and 80 ms, respectively. Spectra were processed with XWINNMR, and they were zero-filled to 4K and 1K points in F_2 and F_1, respectively; squared sine bell functions were applied in both dimensions.

The same NMR experiments were conducted in 40% TFE at 10 °C for the EINbsite and EINosite peptides. HPr$^{9-30}$ has been previously assigned in aqueous and 40% TFE solutions.[32] We did not conduct experiments in the presence of TFE with the Phage peptides because TFE titrations followed by CD did not show sigmoidal curves (data not shown).

Measurements of T_2 (transverse relaxation time). Measurements of T_2 provide a convenient method for assessing binding.[33] We measured the T_2 values of several mixtures of peptides with the corresponding proteins. Experiments were conducted at 25 °C in 50 mM phosphate buffer (pH 7.0). The T_2 measurements were conducted by using the 1-1 echo sequence (at echo times of 2.9 ms and 400 μs).[34] The width of an isolated tryptophan or amide proton resonance was used to measure the T_2; its variation, as the concentration of one of the components of the mixture in the complex was increased, was fit to a 1:1 binding model,[33] according to the equation

$$Y_{obs} = 0.5 Y_{max} \left\{ 1 + X + \frac{K_D}{[\text{macromolecule}]_0} - \left[\left(1 + X + \frac{K_D}{[\text{macromolecule}]_0} \right)^2 - 4X \right]^{1/2} \right\} \quad (4)$$

where X is the molar ratio of the ligand to the macromolecule, Y is the physical magnitude that is being monitored (which can be the chemical shift, the intensity of the signals, or the relaxation times, as in this work) at each different concentration of the ligand added, and $[\text{macromolecule}]_0$ is the concentration of the polypeptide chain that is kept constant throughout the titration experiment.

2D ^{15}N HSQC NMR Spectra. Spectra of wild-type ^{15}N-labeled HPr^{sc} were acquired in the phase-sensitive mode; frequency discrimination in the indirect dimensions was achieved by using the echo/antiecho-TPPI method. The 2D ^{15}N HSQC experiments[35] were conducted with 4K data points in the ^{1}H dimension and 200 scans in the ^{15}N axis. The spectral widths were 15 and 35 ppm in the ^{1}H and ^{15}N dimensions, respectively. Water was suppressed with the WATERGATE sequence.[30] The concentration of HPr^{sc} was 110 μM, and the corresponding EINosite and EINbsite concentration was 4 times higher. For the experiments with the EINbsite/EINosite mixture, the concentration of each peptide was the same (400

dx.doi.org/10.1021/bi3010494 | Biochemistry 2012, 51, 7393−7402

μM). Spectra were acquired at 25 °C in 50 mM phosphate buffer (pH 7.0).

Translational Diffusion NMR Experiments (DOSY). Translational self-diffusion measurements were performed with the pulsed-gradient spin-echo sequence for Phage1, Phage2, EINbsite, and EINosite peptides; DOSY measurements have been previously taken for HPr^{9-30}.[32] The following relationship exists between the translational self-diffusion constant, D, and the delays during acquisition:[36] $I/I_0 = \exp[D\gamma_H^2\delta^2G^2(\Delta - \delta/3 - \tau/2)]$, where I is the measured peak intensity of a particular (or a group of) resonance(s), I_0 is the maximal peak intensity of the same resonance(s) at the smaller gradient strength, D is the translational self-diffusion constant (in $cm^2\ s^{-1}$), δ is the duration (in seconds) of the gradient, G is the gradient strength (in teslas per centimeter), Δ is the time (in seconds) between the gradients, γ_H is the gyromagnetic constant of the proton, and τ is the recovery delay between the bipolar gradients (100 μs in our experiments). Data are plotted as I/I_0 versus G^2, and the exponential factor of the resulting curve is $D\gamma_H^2\delta^2(\Delta - \delta/3 - \tau/2)$, from which D can be easily obtained. The duration of the gradient was varied between 1.8 and 2.5 ms, and the time between both gradients was 150 ms in all peptides. The methyl groups between 0.8 and 1 ppm were used for integration in all peptides. The gradient strength was calibrated by using the value of D for the residual proton water line in a sample containing 100% D_2O in a 5 mm tube.[36] It is important to indicate at this stage that the determined D for each peptide is the weighted average of the translational diffusion coefficients of all species present in the solution. The averaged hydrodynamic radius, R_h, was obtained by assuming that the R_h of dioxane is 2.12 Å.[37] DOSY measurements with each peptide were repeated twice; the reported D value is the average of these two measurements. The peptide concentration was ~2 mM, and the required amount of the lyophilized biomolecule was dissolved in 100% D_2O.

Inhibition Tests. *S. coelicolor* CECT 3243 was used for testing the antimicrobial activity of the peptides used in the work, with antibiotic susceptibility disks. Liquid and solid ISP2 medium (0.4% glucose, 0.4% yeast extract, 1% malt extract) was used for the maintenance and growth of the microorganism, using standard protocols.[38]

Sterile disks were impregnated with 5 μL of the desired compound [water, Phage1 (80 μM) and Phage2 (80 μM), EINosite (300 μM) and EINbsite (400 μM), HPr^{9-30} (150 μM) and kanamycin (142.3 mM, 50 mg/mL) and ampicillin (101.3 mM, 50 mg/mL)]. They were allowed to dry for 2 h before being placed in agar plates with ISP2 medium streaked with 100 μL of liquid culture of *S. coelicolor* CECT 3243 (10^6 colony-forming units). The plates were then incubated overnight at 28 °C. Experiments were repeated four times.

RESULTS

Phage1, Phage2, EINbsite, and EINosite Peptides Were Monomeric and Disordered in Solution. The R_h values experimentally determined from DOSY experiments were similar, within error, to those calculated theoretically for monomeric disordered peptides,[39] according to the expression $R_h = R_0M^v$, where $R_0 = 0.027 \pm 0.01$ nm and $v = 0.50 \pm 0.01$ (Table 1). Therefore, we can conclude that the peptides populate a monomeric random-coil conformation.

The far-UV CD spectra in aqueous solution of the four peptides had minima between 200 and 205 nm, further suggesting that they were mainly disordered (data not shown).

Table 1. Hydrodynamic Measurements of the Peptides

peptide[a]	R_h (Å)[b] ($D \times 10^6$, $cm^2\ s^{-1}$)	R_h (Å)[c]
Phage1 (1716.0)	7 ± 2 (2.4 ± 0.3)	11 ± 3
Phage2 (1151.4)	6 ± 2 (2.7 ± 0.3)	9 ± 2
EINosite (2209.4)	12.3 ± 0.8 (8.29 ± 0.04)	12 ± 2
EINbsite (1843.0)	9.8 ± 0.7 (9.49 ± 0.01)	11 ± 3

[a]The mass of each peptide is within the parentheses (in daltons). [b]Determined from DOSY measurements. The errors in D are the average of the fitting errors of two measurements. Errors in R_h are propagation errors. [c]Determined by the equation of Danielsson and co-workers.[38]

We assigned the four peptides in aqueous solution, by using homonuclear NMR standard methods.[31] Several lines of evidence confirmed that the peptides did not have a well-defined conformation. First, no long- or medium-range NOEs were detected (Figure 1A–D), neither were short-range [i.e., (i, i + 2)] or medium-range [(i, i + 3) and (i, i + 4)] NOEs detected. Second, the sequence-corrected conformational shifts[31,40] for any of the peptide Hα protons were within the commonly accepted range for random-coil peptides ($|\Delta\delta| \leq 0.1$ ppm) (Tables S1–S4 of the Supporting Information); only the conformational shifts of the N- and C-terminal residues or those of residues following an aromatic amino acid showed a deviation from that interval.

We also conducted NMR experiments in the presence of 40% TFE for EINbsite and EINosite (Tables S5 and S6 of the Supporting Information), because some of their residues were involved in the α-helices in the whole EIN^{sc} (the C-terminus in EINbsite and both termini in EINosite). At that TFE concentration, the sigmoidal titration of both peptides (representing the coil ↔ ordered structure reaction) has finished, and the curve has reached a plateau (data not shown). The results suggest that whereas EINbsite (Figure 1A of the Supporting Information) had NN(i, i + 1) and medium-range NOEs at the C-terminus, EINosite did not show any evidence of medium-range NOEs (Figure 1B of the Supporting Information); therefore, the EINosite peptide does not have a strong tendency to acquire a helical conformation. This behavior contrasts with that observed in HPr^{9-30}, where a fully formed helix was observed in the presence of the cosolvent.[32]

Phage1 and Phage2 Peptides Were Bound to EIN^{sc} with a High Affinity. First, we assessed the binding by measurements of the T_2 relaxation time. As there is a tryptophan in Phage1 and EIN lacks tryptophan residues, we followed the changes in the T_2 relaxation time of that indole signal as the EIN^{sc} concentration was increased (with a constant Phage1 concentration of 100 μM); the equilibrium was fast on the NMR time scale because a single set of signals was observed for the indole proton of Phage1. As the EIN^{sc} concentration was increased, the T_2 relaxation time was reduced, as a larger population of the EIN^{sc}–Phage1 complex (with a higher molecular weight) was present (Figure 2A). On the other hand, because Phage2 has no isolated signals (Table S2 of the Supporting Information), we followed the changes in the T_2 relaxation time of the protons at 10.30 ppm of EIN^{sc} (which correspond to two amide protons[24]). In this case, the equilibrium was also fast on the NMR time scale, but as the Phage2 concentration was increased ([EIN^{sc}] = 95 μM), the T_2 increased, because a larger proportion of the EIN^{sc}–Phage2 complex was present (Figure 2B). It is important to note that variations in T_2 for the Phage2–EIN^{sc} complex were smaller

Figure 1. Summary of structural data for (A) Phage1, (B) Phage2, (C) EINbsite, and (D) EINosite peptides in aqueous solution. NOEs are classified as strong, medium, or weak according to the height of the bar underneath the sequence. Intensities were judged by visual inspection from the NOE contacts measured in the ROESY experiment. The corresponding Hα NOEs with the following Hδ of a proline residue are indicated by an empty bar in the row corresponding to the αN(i, i + 1) contacts. The dotted lines indicate NOE contacts that could not be unambiguously assigned because of signal overlap. The numbering of EINbsite and EINosite peptides corresponds to that of the whole sequence of EIN^{sc}.

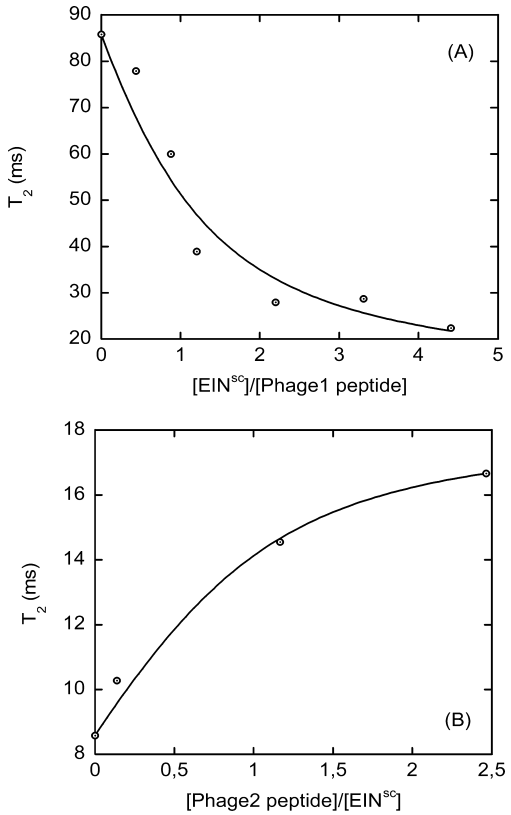

Figure 2. Affinity of the Phage peptide−EIN^{sc} complexes as measured by NMR. (A) Variation of T_2 of the indole proton of Phage1 upon addition of EIN^{sc}. (B) Variation of the signals at 10.30 ppm in EIN^{sc} upon addition of Phage2. Experiments were conducted at 25 °C in 50 mM phosphate buffer (pH 7.0). The curves were the fittings to a 1:1 binding model (eq 4) according to Fielding.[33]

than for the other complex, because of the different signals observed in the two complexes (in the Phage1 complex we observed that of the peptide and in the Phage2 complex that of EIN^{sc}). We determined the K_D from the variation of the T_2 relaxation time in both peptides (Figure 2). The values were 65 ± 56 μM for Phage1 and 31 ± 20 μM for Phage2.[33]

Second, we determined quantitatively the binding by ITC (Table 2 and Figure 3A−C). To allow for a comparison, we measured (i) the K_D of the EIN^{sc}−HPr$^{9-30}$ complex, which was ~8 μM, 30 times smaller than that obtained for the EI^{sc}−HPr$^{9-30}$ complex (~200 μM[21]), and (ii) the K_D of the EIN^{sc}−HPr^{sc} complex (~12 μM). The K_D of the EIN^{sc} complexes with Phage1 and Phage2 peptides were 2 times smaller (Table 2), and they were similar, within error, to those determined by NMR (see above). The values of the binding enthalpies and entropies indicate that the processes were entropically driven; the ΔC_p values were negative, as expected. A positive value of n_H indicates a protonation, the uptake of a proton by the complex, as occurred in the EIN^{sc}−HPr$^{9-30}$ complex (Table 2), where the number of exchanged protons was close to 0.5; a positive value of n_H was also obtained for the EIN^{sc}−HPr^{sc} complex (0.52). On the other hand, a negative value of n_H indicates a deprotonation, the release of a proton from a residue in the complex; the values of n_H were smaller and negative in both Phage peptides.

EINbsite and EINosite Peptides Bound HPr^{sc} with a Lower Affinity than Phage1 and Phage2. First, we determined qualitatively the binding by measuring the T_2 relaxation time of an isolated signal at 9.49 ppm in the spectrum of HPr^{sc}. In the presence of the peptides, T_2 increased from 26.8 to 35.3 ms at a 1:2 HPr^{sc}:EIN peptide ratio; attempts to obtain a titration curve like those in Phage peptides (Figure 2) failed, probably because of the smaller size of HPr^{sc} compared to EIN^{sc}. Therefore, we tried to further confirm the presence of binding by mapping the changes (in chemical shifts and/or in signal intensities) in the HSQC spectra of HPr^{sc} (Figure 2 of the Supporting Information). Upon addition of EINsite peptide, there were signals that showed variations in intensity and/or in some chemical shifts. Therefore, both NMR experiments suggest that there was binding between EINsite peptides and HPr^{sc}.

The affinities of both EINsite peptides for HPr^{sc} were determined by using ITC. The K_D values of the complexes involving HPr^{sc} with the EIN^{sc}-derived peptides were 2 times higher than those with the Phage peptides or HPr$^{9-30}$ (Table 2 and Figure 3D,E); furthermore, the K_D of HPr^{sc} with equimolar amounts of both EIN^{sc}-derived peptides was similar to those of the complexes involving the isolated peptides (Table 2 and Figure 3F). As in the Phage peptides, the binding was entropically driven.

The Peptides Have Activity in Vivo. The assays in vivo have shown that all peptides, except EINosite, had antimicrobiological activity against *S. coelicolor* CECT 3243 (Figure 4); even Phage1 and Phage2, which were originally designed against *E. coli*, showed activity similar to that shown by the rest of the peptides. The reasons behind the absence of activity in EINosite are not understood, but it could be due to the lack of a sufficient peptide concentration or, more probably, to the fact that it is the only peptide that does not contain the active-site histidine (see above).

dx.doi.org/10.1021/bi3010494 | *Biochemistry* 2012, 51, 7393−7402

Table 2. Thermodynamic Parameters for the Binding Reactions As Determined by ITC[a]

complex	K_D (μM)	$\Delta H°$ (kcal/mol)[b]	ΔC_p (kcal/mol)[c]	$\Delta G°$ (kcal/mol)[d]	$-T\Delta S°$ (kcal mol^{-1} K^{-1})[e]	n_H[f]
EIN^{sc}–HPr$^{9-30}$	8.4	10.7	−0.25	−6.9	−17.6	0.49
EIN^{sc}–Phage1	5.1	−0.3	−0.12	−7.2	−6.9	−0.30
EIN^{sc}–Phage2	4.3	0.1	−0.05	−7.3	−7.4	−0.08
HPr^{sc}–EINbsite	18	1.4	0.03	−6.4	−7.8	−0.26
HPr^{sc}–EINosite	14	1.5	−0.05	−6.6	−8.1	−0.18
HPr^{sc}–(EINbsite + EINosite)	16	1.5	*g*	−6.5	−8.0	−0.25

[a]All titrations were conducted in 10 mM Tris buffer (pH 7.0) at 25 °C. K_D is the dissociation constant. Typical relative errors are 20–25% for K_D, <5% for $\Delta G°$, 5–10% for $\Delta H°$ and $-T\Delta S°$, 20% for ΔC_p, and 10% for n_H. Experiments were conducted in duplicate. [b]The value of the buffer-independent enthalpy for the binding reaction was determined by conducting experiments in 10 mM Tris and Mops buffers (pH 7.0) at 25 °C, and by using eq 1. [c]The heat capacity of the binding reaction was determined by conducting experiments in 10 mM Tris buffer (pH 7.0) at 15, 25, and 35 °C, for all the reactions except those involving Phage1 and Phage2 peptides, where the 10 mM Mops buffer (pH 7.0) at 15 and 25 °C was used. In all cases, a linear relationship between the value of the enthalpy of binding and the temperature was observed, in agreement with a well-defined constant binding heat capacity over the temperature range considered (15–35 °C). [d]$\Delta G°$ is the binding free energy at 25 °C, determined as $\Delta G° = RT \ln K_D$. [e]The value of the entropic contribution of the binding reaction at 25 °C, determined as $-T\Delta S° = \Delta G° - \Delta H°$. [f]The number of exchanged protons, determined by conducting experiments in 10 mM Tris and Mops buffers (pH 7.0) at 25 °C, by using eq 1. [g]This value was not determined because of the nonlinearity of ΔH vs temperature, and the large associated errors when attempts to fit the data to several polynomial equations were used.

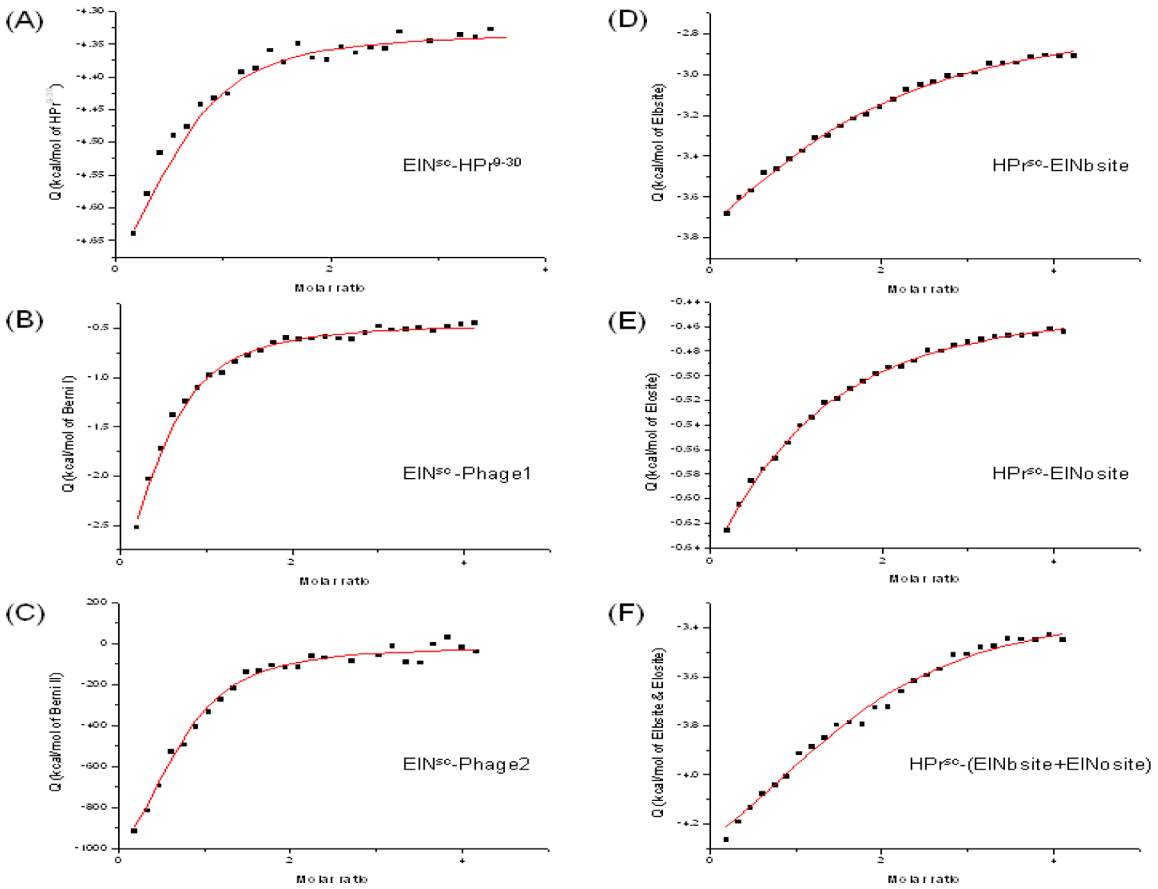

Figure 3. Determination of the affinity constants of the complexes by ITC. The fitting curves were obtained assuming a 1:1 model. (A–C) Binding of HPr$^{9-30}$ and Phage peptides to EIN^{sc}. (D–F). Binding of EINsite peptides to HPr^{sc}.

DISCUSSION

Affinity of the Peptides for EIN^{sc} and Their Acquisition of Nativelike Structure. A favorable binding entropy indicates that water molecules are expelled from the complex interface, and this represents a main driving force counterbalancing the conformational and roto-translational entropic losses.[28] These results differ from those of the association of the whole EI^{sc} with HPr^{sc}, which was enthalpy-driven.[21] Furthermore, the K_D of the EIN^{sc}–HPr$^{9-30}$ complex (~8 μM) was smaller than those for the EI^{sc}–HPr$^{9-30}$ (~200 μM)[21] and EIN^{sc}–HPr^{sc} (~12 μM) complexes. These differences might arise from the presence of the EIC, because binding of HPr$^{9-30}$ probably requires dissociation of the dimeric EI^{sc} (as it happens when the entire HPr^{sc} binds to EI^{sc}).

The measured enthalpies show differences among the species assayed (Table 2); in fact, the binding enthalpy for the EIN^{sc}–HPr$^{9-30}$ complex was similar to that measured for the EI^{sc}–HPr$^{9-30}$ complex, suggesting that the differences in the affinities must rely on entropic considerations and, therefore, in the dimeric character of EI^{sc}. The value of $\Delta H°$ is composed of the

dx.doi.org/10.1021/bi3010494 | Biochemistry 2012, 51, 7393–7402

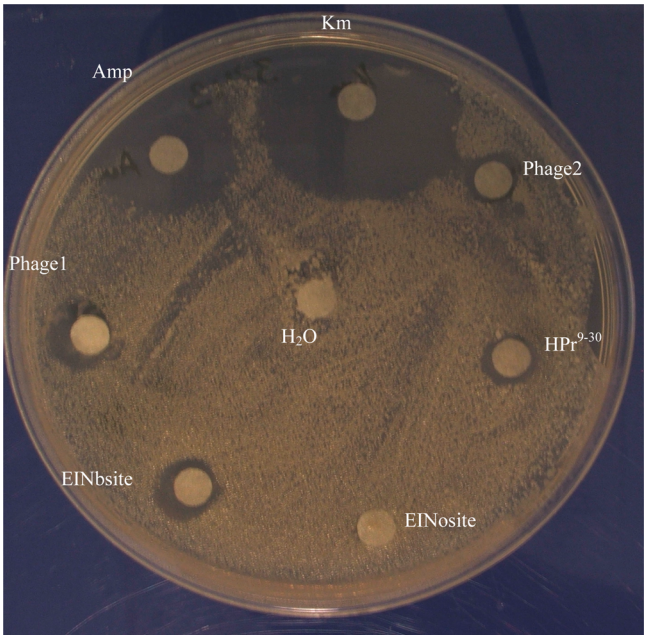

Figure 4. Kirby–Bauer antibiotic testing of the peptides used in this work. The antibiotics kanamycin and ampicillin (50 mg/mL) were used as positive controls, and water was used as a negative control. Note that the concentrations of kanamycin (142.3 mM, 50 mg/mL) and ampicillin (101.3 mM, 50 mg/mL) were 1000 times higher than that of the assayed peptides (in the range of micromolar).

intrinsic binding enthalpy (which is a result of the net balance between formation and breakdown of van der Waals, electrostatic, and hydrogen bond interactions between the binding partners and the solvent) and the ionization enthalpy of the groups involved in the proton exchange from the two molecules of the complex (protein and peptide). The value of $\Delta H°$ for the EIN^{sc}–HPr$^{9-30}$ complex is the highest, suggesting a protonation during the binding reaction,[28] as it is also supported by the calculation of n_H (Table 2). Conversely, the formation of the Phage1 and Phage2 complexes showed a small deprotonation (Phage1) and no net proton transfer (Phage2); therefore, the mechanism of binding seems to be different among the species assayed, although in all of them, it resulted in the burial of hydrophobic surfaces [because ΔC_p values were negative (Table 2)]. On the other hand, the mechanism of binding seems also to be different from that previously reported for the EI^{sc}–HPr$^{9-30}$ complex, where a stronger deprotonation upon complex formation was observed ($n_H = -0.96$).[21]

We have previously observed, by using STD-NMR measurements, that binding of EI^{sc} to HPr$^{9-30}$ involved acquisition of a helical nativelike structure of the peptide. Attempts to conduct STD-NMR measurements with the EIN^{sc}–HPr$^{9-30}$ complex were unsuccessful, probably because of the smaller size of EIN^{sc} compared to EI^{sc}. Therefore, we should infer that the same helixlike structure in HPr$^{9-30}$ is acquired upon binding to EIN^{sc}. Interestingly enough, Phage1 and Phage2 peptides have no intrinsic tendency to form helical structure [as suggested by prediction programs and by TFE titrations conducted in our laboratories (data not shown)]; therefore, binding to EIN^{sc} of those peptides does not involve the acquisition of helical nativelike structure around the active-site histidine. This is further supported by the fact that attempts to assess the binding by CD measurements (which led to successful results in assessing the binding of EI^{sc} to HPr$^{9-30}$ [21]) did not yield variations in the ellipticity of the complex spectra when compared to that of the spectrum of the isolated EIN^{sc} (data not shown).

Affinity of the Designed Peptides for HPr^{sc} and Their Acquisition of Nativelike Structure. Whereas EINbsite comprises the active-site region of EIN^{sc} and EINosite involves the region of EIN^{sc} close to the active site of HPr^{sc}, the affinity of both peptides was the same, within error (Table 2); however, the binding mechanisms were different as judged by the dissimilar ΔC_p values. This dissimilar binding mechanism was further supported by the fact that the signals in the HSQC spectra of HPr^{sc} affected by the two isolated peptides were different (Figure 2 of the Supporting Information); the positive value of ΔC_p for EINbsite binding further suggests solvent exposure of the hydrophobic surface upon binding. On the other hand, the use of a "cocktail" mixture of both peptides did not show a large variation in the affinity, suggesting that there is not a synergic effect of both peptides on HPr^{sc}. The absence of a synergic effect could imply that (i) other regions of EIN^{sc} are needed to bind strongly to HPr^{sc}, (ii) both peptides are mutually excluding, or (iii) they bind in an independent fashion. With regard to the thermodynamic parameters of formation of the HPr^{sc}–(EINbsite + EINosite) complex, the nonlinearity of ΔH versus temperature might be due to large conformational rearrangements upon binding or, alternatively, to the pre-existence of a temperature-dependent conformational equilibrium.[41] The dissociation constant of EINbsite is 18 μM, and that for EINosite is very similar, 14 μM. The binding enthalpies of these two peptides are also similar, around 1.5 kcal/mol. In the titration with the peptide mixture, a dissociation constant of 16 μM is obtained, which is close to the geometric mean of the individual dissociation constants, and also the binding enthalpy is the arithmetic mean of the individual binding enthalpies. This finding is in agreement with the hypothesis of independent mutually exclusive binding of both peptides. If both peptides could bind simultaneously and independently, we would expect an observed binding enthalpy equal to the sum of the individual binding enthalpies. On the other hand, if both peptides could bind simultaneously and cooperatively (positive or negative cooperativity), we would expect an observed dissociation constant different from that obtained experimentally.

The affinities of the EINsite peptides for HPr^{sc} were similar to that of the EIN^{sc}–HPr^{sc} complex, suggesting that even though they do not contain the full binding region of EIN^{sc}, most of the energetically important regions in binding are present in those peptides. However, inhibition in vivo was observed for only the EINbsite peptide, suggesting that the presence of the active-site histidine might be important for achieving activity (Figure 4). Furthermore, because these peptides did not exhibit a strong intrinsic tendency to form helical structure [as concluded from the experiments in the presence of TFE (Figure 1 of the Supporting Information)], we suggest that (i) nativelike helical structure in the peptides is not necessary to achieve binding and probably (ii) upon binding to HPr^{sc} the peptides do not acquire a fully, well-defined, nativelike structure (as it occurs in the Phage peptides).

Finally, it could be thought that peptide binding involved the unspecific presence of several molecules of the peptide for a single molecule of the PTS protein. We have several pieces of evidence suggesting that the complexes form a specific complex with a 1:1 stoichiometry with either EIN^{sc} or HPr^{sc}. First, the measurements of the relaxation time for the complexes allow

dx.doi.org/10.1021/bi3010494 | Biochemistry 2012, 51, 7393–7402

the estimation of the molecular mass of the complexes; when the rate of both molecules ([peptide] to [PTS protein]) equals 1, the calculated mass of the complex is close to that expected from the addition of the masses of the isolated polypeptide chains. Furthermore, in the range of concentrations explored, the calculated masses of the complexes did not involve a stoichiometry of 2:1 ([peptide]/[PTS protein]) or higher. Second, the 1:1 stoichiometry equation (eq 4) fits well the T_2 relaxation data (Figure 2). Third, we fit the ITC binding isotherms to several stoichiometries (peptide:protein), and in all cases, the fittings were worse or had a χ^2 similar to that obtained for the 1:1 stoichiometry; therefore, we used Occam's razor criteria to choose the simplest model. Finally, the binding is not unspecific, because only some particular signals in the NMR spectra are modified upon peptide addition (Figure 2 of the Supporting Information), and among them, in our partial assignment for HPr^{sc}, we observed His15, the active-site histidine.

Biological Implications. Bacterial pathogens are becoming increasingly resistant to the antibiotics used to tackle infectious diseases. More than 150 antibiotics belonging to at least 17 different classes are now available. Each antibiotic operates at a specific site within the cell. Some of them inhibit the cell wall synthesis (as β-lactams). Others disorganize cell membranes (such as polymixins). Others inhibit the protein synthesis (such as chloramphenicol), DNA or RNA. Others target particular biochemical pathways (such as methotrexate in the synthesis of folic acid). However, the increasing resistance makes more compelling than ever the search for new targets.[42] Here we propose the first phosphorylation step in PTS as a drug target. Our strategy is different from that using PTS transporters as vehicles for antibiotic uptake[43] or the use of PEP as antibacterials.[44] Our methodology involves the inhibition of the first phosphorylation step within the PTS cascade by using the two general proteins as targets. We used a rational approach to target the protein−protein interaction (PPI) interface of the EIN^{sc}−HPr^{sc} complex, based on (i) the structure of the determined complex in other bacterial species and (ii) combinatorial and phage display approaches against EI^{ec} developed by other authors.[22,23]

The first conclusion of our work is that the designed peptides (based on short fragments comprising the active sites and nearby regions in both proteins) can be considered good hit compounds, because their affinities for the target proteins are similar to that measured (12 μM) in the complex of both intact proteins (EIN^{sc}−HPr^{sc}). Thus, we may conclude that the protein−protein interface of this complex is druggable, even though the interfaces of both proteins are very large.[12] Moreover, the intrinsic binding affinities for the peptides could be even higher, because the observed binding affinity contains an energetic penalty due to the conformational restriction upon binding; therefore, conformationally restricted ligands derived from these peptides might exhibit higher binding affinities.

The second conclusion of our studies stems from the use of peptides with no relationship to EI^{sc}, and designed for inhibiting EI^{ec}. Phage1 and Phage2 had the smallest K_D values (Table 2). Therefore, peptides that are not sequence-related to EI^{sc} or HPr^{sc} showed the highest affinities. Interestingly enough, both Phage1 and Phage2 peptides were designed against the EI^{ec};[22,23] these results suggest that peptides designed against a PTS protein in a species may be active against the homologous protein from another species, thus allowing the interspecies jump.

Finally, our studies show that although the PPI of the EIN^{sc}−HPr^{sc} complex mainly involves α-helices from both proteins (close to the active sites), the Phage1, Phage2, and EINsite peptides did not show a significant tendency to acquire a helical nativelike structure, and they did bind to the protein target with an affinity comparable to that of the intact protein (Table 2). However, our studies suggest that although native structure does not seem to be important to achieve binding (Figure 3) and inhibition in vivo (Figure 4), the presence of the active-site histidine might be a key residue allowing antimicrobial activity in vivo. Therefore, we suggest that various chemotypes can bind effectively to both PTS proteins, and thus, the possible hit compounds do not need to exactly mimic the natural target of the EI−HPr interface. These results indicate that several scaffolds might be effective for disrupting this particular PPI.

■ ASSOCIATED CONTENT

Supporting Information

NOE schemes of EINbsite and EINosite in the presence of 40% TFE (Figure 1), HSQC spectra of HPr^{sc} with EINbsite, EINosite, and the EINbsite/EINosite mixture (Figure 2), and six tables listing the NMR assignments of Phage1 and Phage2 (in aqueous solution) and EINosite and EINbsite (in aqueous solution and in 40% TFE). This material is available free of charge via the Internet at http://pubs.acs.org.

■ AUTHOR INFORMATION

Corresponding Author

*A.V.-C.: Institute of Biocomputation and Physics of Complex Systems (BIFI), Universidad de Zaragoza, Zaragoza, Spain; telephone, +34 976762996; fax, +34 976762990; e-mail, adrianvc@unizar.es. J.L.N.: Instituto de Biología Molecular y Celular, Universidad Miguel Hernández, Avda. del Ferrocarril s/n, 03202 Elche (Alicante), Spain; telephone, + 34 966658459; fax, +34 966658758; e-mail, jlneira@umh.es.

Author Contributions

R.D. and J.L.N. contributed equally to this work.

Funding

This work was supported by the Spanish Ministerio de Ciencia e Innovación (MCINN) (CTQ2011-24393 and CSD2008-00005 to J.L.N. and BFU2010-19451 to A.V.-C.), Diputación General de Aragón (PI044/09 to A.V.-C.), and intramural BIFI 2011 projects (to A.V.-C. and J.L.N.). S.M.-R. was supported by the Andalusia government. The stays of R.D. in the laboratory of A.V.-C. were supported by the Spanish Ministerio de Ciencia e Innovación (BFU2008-02302-BMC).

Notes

The authors declare no competing financial interest.

■ ACKNOWLEDGMENTS

We thank Prof. Richard N. Armstrong for handling the manuscript. We thank both reviewers for their ideas, helpful discussions, and suggestions. We thank Fritz Titgemeyer for the kind gift of the EI and HPr genes. We deeply thank May García, María del Carmen Fuster, Javier Casanova, and Raquel Jorquera for technical assistance.

■ ABBREVIATIONS

CD, circular dichroism; DSC, differential scanning calorimetry; EI, enzyme I; EI^{sc}, EI from *S. coelicolor*; EI^{ec}, EI from *E. coli*;

EIC, C-terminal region of EI (comprising approximately the last 300 residues); EIC^{sc}, C-terminal region of EI^{sc}; EIN, N-terminal region of EI (comprising approximately the first 250 residues); EIN^{sc}, N-terminal domain (residues 1−246) of EI^{sc}; EIN^{ec}, N-terminal domain of EI^{ec}; EII, enzyme II permease; HPr, histidine phosphocarrier protein; HPr^{sc}, HPr from *S. coelicolor*; HPr^{bs}, HPr from *Bacillus subtilis*; HPr^{ec}, HPr from *E. coli*; ITC, isothermal titration calorimetry; PEP, phosphoenolpyruvate; PTS, PEP-dependent phosphotransferase system; PPI, protein−protein interactions; TFE, 2,2,2-trifluoroethanol; TSP, sodium trimethylsilyl[2,2,3,3-$^{2}H_4$]propionate; UV, ultraviolet.

REFERENCES

(1) Görke, B., and Stülke, J. (2008) Carbon catabolite repression in the bacteria. *Nat. Microbiol. 6*, 613−624.

(2) Deutscher, J., Francke, C., and Postma, P. W. (2006) How phosphotransferase system-related protein phosphorylation regulates carbohydrate metabolism in bacteria. *Microbiol. Mol. Biol. Rev. 70*, 939−1031.

(3) Deutscher, J. (2008) The mechanisms of catabolite repression in bacteria. *Curr. Opin. Microbiol. 11*, 87−93.

(4) Lengeller, J. W., and Jahreis, K. (2009) Bacterial PEP-dependent carbohydrate:phosphotransferase systems couple sensing and global control mechanisms. *Contrib. Microbiol. 16*, 65−87.

(5) Weigel, M., Kukuruzinska, M. A., Nakazawa, A., Waygood, E. B., and Roseman, S. (1982) Sugar transport by the bacterial phosphotransferase system. Phosphoryl transfer reactions catalyzed by enzyme I of *Salmonella typhimurium*. *J. Biol. Chem. 257*, 14477−14491.

(6) Hu, K. Y., and Saier, M. H., Jr. (2002) Phylogeny of phosphoryl transfer proteins of the phosphoenolpyruvate-dependent sugar-transporting phosphotransferase system. *Res. Microbiol. 153*, 405−415.

(7) Lee, B. R., Lecchi, P., Panell, L., Jaffe, H., and Peterkosfsky, A. (1994) Identification of the N-terminal domain of enzyme I of the *Escherichia coli* phosphoenolpyruvate:sugar phosphotransferase system produced by proteolytic digestion. *Arch. Biochem. Biophys. 312*, 121−124.

(8) Zhu, P. P., Szczepanowski, R. H., Nosworthy, N. J., Ginsburg, A., and Peterkofsky, A. (1999) Reconstitution studies using the helical and carboxy-terminal domains of enzyme I of the phosphoenolpyruvate:sugar phosphotransferase system. *Biochemistry 38*, 15470−15479.

(9) Brokx, S. J., Talbot, J., Geroges, F., and Waygood, E. B. (2000) Enzyme I of the phosphoenolpyruvate:sugar phosphotransferase system. *In vitro* intragenic complementation: The roles of Arg126 in phosphoryl transfer and the C-terminal domain in dimerization. *Biochemistry 39*, 3624−3635.

(10) Liao, D. I., Silverton, E., Seok, Y. J., Lee, B. R., Peterkofsky, A., and Davies, D. R. (1996) The first step in sugar transport: Crystal structure of the amino terminal domain of enzyme I of the *E. coli* PEP:sugar phosphotransferase system and a model of the phosphotransfer complex with HPr. *Structure 4*, 861−872.

(11) Garrett, D. S., Seok, Y. K., Liao, D. I., Peterkofsky, A., Gronenborn, A. M., and Clore, G. M. (1997) Solution structure of the 30 kDa N-terminal domain of enzyme I of the *Escherichia coli* phosphoenolpyruvate:sugar phosphotransferase system by multidimensional NMR. *Biochemistry 36*, 2517−2530.

(12) Garrett, D. S., Seok, Y. K., Peterkofsky, A., Gronenborn, A. M., and Clore, G. M. (1999) Solution structure of the 40,000 Mr phosphoryl transfer complex between the N-terminal domain of enzyme I and HPr. *Nat. Struct. Biol. 6*, 166−173.

(13) Teplyakov, A., Lim, K., Zhu, P.-P., Kapadia, G., Chen, C. C. H., Schwartz, J., Howard, A., Reddy, P. T., Peterkofsky, A., and Herzberg, O. (2006) Structure of the phosphorylated enzyme I, the phosphoenolpyruvate:sugar phosphotransferase system sugar translocation protein. *Proc. Natl. Acad. Sci. U.S.A. 103*, 16218−16223.

(14) Parche, S., Schmid, R., and Titgemeyer, F. (1999) The phosphotransferase system (PTS) of *Streptomyces coelicolor*. Identification and biochemical analysis of a histidine phosphocarrier protein HPr encoded by the gene ptsH. *Eur. J. Biochem. 265*, 308−317.

(15) Nothaft, H., Dresel, D., Willimek, A., Mahr, K., Niederweis, M., and Titgemeyer, F. (2003) The phosphotransferase system of *Streptomyces coelicolor* is biased for N-acetylglucosamine metabolism. *J. Bacteriol. 185*, 7019−7023.

(16) Nothaft, H., Parche, S., Kamionka, A., and Titgemeyer, F. (2003) *In vivo* analysis of HPr reveals a fructose-specific phosphotransferase system that confers high-affinity uptake in *Streptomyces coelicolor*. *J. Bacteriol. 85*, 929−937.

(17) Fernández-Ballester, G., Maya, J., Martin, A., Parche, S., Gómez, J., Titgemeyer, F., and Neira, J. L. (2003) The histidine-phosphocarrier protein of *Streptomyces coelicolor* folds by a partially folded species at low pH. *Eur. J. Biochem. 270*, 2254−2267.

(18) Neira, J. L., and Gómez, J. (2004) The conformational stability of the *Streptomyces coelicolor* histidine-phosphocarrier protein. Characterization of cold denaturation and urea-protein interactions. *Eur. J. Biochem. 271*, 2165−2181.

(19) Hurtado-Gómez, E., Barrera, F. N., and Neira, J. L. (2005) Structure and conformational stability of the enzyme I of *Streptomyces coelicolor* explored by FTIR and circular dichroism. *Biophys. Chem. 115* (2−3), 229−233.

(20) Hurtado-Gómez, E., Fernández-Ballester, G., Nothaft, H., Gómez, J., Titgemeyer, F., and Neira, J. L. (2006) Biophysical characterization of the Enzyme I of the *Streptomyces coelicolor* phosphoenolpyruvate:sugar phosphotransferase system. *Biophys. J. 90*, 4592−4604.

(21) Hurtado-Gómez, E., Abián, O., Muñoz, F. J., Hernáiz, M. J., Velázquez-Campoy, A., and Neira, J. L. (2008) Defining the epitope region of a peptide from the *Streptomyces coelicolor* phosphoenolpyruvate:sugar phosphotransferase system able to bind to the Enzyme I. *Biophys. J. 95*, 1336−1348.

(22) Mukhija, S., Germeroth, L., Schneider-Mergener, J., and Erni, B. (1998) Identification of peptides inhibiting enzyme I of the bacterial phosphotransferase system using combinatorial cellulose-bound peptide libraries. *Eur. J. Biochem. 254*, 433−438.

(23) Mukhija, S., and Erni, B. (1997) Phage display selection of peptides against enzyme I of the phosphoenolypyruvate-sugar phosphotransferase system (PTS). *Mol. Microbiol. 25*, 1159−1166.

(24) Romero-Beviar, M., Martínez-Rodríguez, S., Prieto, J., Goormaghtigh, E., Ariz, U., Martínez-Chantar, M., Gómez, J., and Neira, J. L. (2010) The N-terminal domain of the Enzyme I is a monomeric well-folded protein with a low conformational stability and residual structure in the unfolded state. *Protein Eng., Des. Sel. 23*, 729−742.

(25) Miroux, B., and Walker, J. E. (1996) Over-production of proteins in *Escherichia coli*: Mutant hosts that allow synthesis of some membrane proteins and globular proteins at high levels. *J. Mol. Biol. 260*, 289−298.

(26) Alcaraz, L. A., del Alamo, M., Barrera, F. N., Mateu, M. G., and Neira, J. L. (2007) Flexibility in HIV-1 assembly subunits: Solution structure of the monomeric C-terminal domain of the capsid protein. *Biophys. J. 93*, 1264−1276.

(27) Gill, S. C., and von Hippel, P. H. (1989) Calculation of protein extinction coefficients from amino acid sequence data. *Anal. Biochem. 182*, 319−326.

(28) Hinz, H. J., Shiao, D. D. F., and Sturtevant, J. M. (1971) Calorimetric investigation of inhibitor binding to rabbit muscle aldolase. *Biochemistry 10*, 1347−1352.

(29) Wishart, D. S., Bigam, C. G., Yao, J., Abildgaard, F., Dyson, H. J., Oldfield, E., Markley, J. L., and Sykes, B. D. (1995) ^{1}H, ^{13}C and ^{15}N chemical shift referencing in biomolecular NMR. *J. Biomol. NMR 6*, 135−140.

(30) Piotto, M., Saudek, V., and Sklenar, V. (1992) Gradient-tailored excitation for single-quantum NMR spectroscopy of aqueous solutions. *J. Biomol. NMR 2*, 661−665.

(31) Wüthrich, K. (1986) *NMR of nucleic acids and proteins*, Wiley & Sons, New York.
(32) Hurtado-Gómez, E., Caprini, M., Prieto, A., and Neira, J. L. (2007) The helical structure propensity in the first helix of the histidine phosphocarrier protein of *Steptomyces coelicolor*. *Protein Pept. Lett. 14*, 281−290.
(33) Fielding, L. (2007) NMR methods for the determination of protein-ligand dissociation constants. *Prog. Nucl. Magn. Reson. Spectrosc. 51*, 219−242.
(34) Sklenar, V., and Bax, A. (1987) Spin echo water suppression for the generation of pure-phase two-dimensional NMR spectra. *J. Magn. Reson. 74*, 469−479.
(35) Bodenhausen, G., and Ruben, D. (1980) Natural abundance nitrogen-15 NMR by enhanced heteronuclear spectroscopy. *Chem. Phys. Lett. 69*, 185−189.
(36) Czypionka, A., de los Paños, O. R., Mateu, M. G., Barrera, F. N., Hurtado-Gómez, E., Gómez, J., Vidal, M., and Neira, J. L. (2007) The isolated C-terminal domain of Ring1B is a dimer made of stable, well-structured monomers. *Biochemistry 46*, 12764−12776.
(37) Wilkins, D. K., Grimshaw, S. B., Receveur, V., Dobson, C. M., Jones, J. A., and Smith, L. J. (1999) Hydrodynamic radii of native and denatured proteins measured by pulse field gradient NMR techniques. *Biochemistry 38*, 16424−16431.
(38) Kieser, T., Bibb, M. J., Buttner, M. J., Chater, K. F., and Hopwood, D. A. (2000) *Practical Streptomyces Genetics*, John Innes Foundation, Norwich, U.K.
(39) Danielson, J., Jarvet, J., Damberg, P., and Gräslund, A. (2002) Translational diffusion measured by PFG-NMR on full length and fragments of the Alzheimer Aβ(1−40) peptide. Determination of hydrodynamic radii of random coil peptides of varying length. *Magn. Reson. Chem. 40*, S89−S97.
(40) Schwarzinger, S., Kroon, G. J. A., Foss, T. R., Chung, J., Wright, P. E., and Dyson, H. J. (2001) Sequence-dependent correction of random coil NMR chemical shifts. *J. Am. Chem. Soc. 123*, 2970−2978.
(41) Jelesarov, I., and Bosshard, H. R. (1999) Isothermal titration calorimetry and differential scanning calorimetry as complementary tools to investigate the energetics of biomolecular recognition. *J. Mol. Recognit. 12*, 3−18.
(42) Fischbach, M. A., and Walsh, C. T. (2009) Antibiotics for emerging pathogens. *Science 325*, 1089−1093.
(43) Parr, T. R., and Saier, M. H., Jr. (1992) The bacterial phosphotransferase system as a potential vehicle for the entry of novel antibiotics. *Res. Microbiol. 143*, 443−447.
(44) Cordaro, J. C., Melton, T., Stratis, J. P., Atagun, M., Gladding, C., Hartaman, P. E., and Roseman, S. (1976) Fosfomycin resistance: Selection method for internal and extended deletions of the phosphoenolpyruvate:sugar phosphotransferase genes of *Salmonella typhimurium*. *J. Bacteriol. 128*, 785−793.